Biometals (2008) 21:41–51
DOI 10.1007/s10534-007-9091-x

Synthesis and biological activity of saccharide based lipophilic siderophore mimetics as potential growth promoters for mycobacteria

Peter Gebhardt · Alvin L. Crumbliss · Marvin J. Miller · Ute Möllmann

Received: 7 December 2006 / Accepted: 19 February 2007 / Published online: 28 March 2007

Abstract Siderophores based on sugar backbones substituted at the 2,3,4- or 2,3,6 positions with hydroxamic or retro-hydroxamic acid chelating units were synthesized and characterized. The alkyl terminus of the iron-coordinating side chain units facilitate lipophilic interactions. Iron coordination properties and complex stability were investigated by ESI-MS and the CAS-Test. The results were correlated to structure activity relationships determined by microbial growth promotion studies under iron limited conditions using wild type strains and iron transport mutants of *Mycobacterium smegmatis*.

P. Gebhardt
Biomolecular Chemistry, Leibniz Institute for Natural Products Research and Infection Biology – Hans-Knoell-Institute, Beutenbergstrasse 11a, 07745 Jena, Germany

A. L. Crumbliss
Department of Chemistry, Duke University, Durham, NC 27708-0346, USA

M. J. Miller
Department of Chemistry and Biochemistry, University of Notre Dame, 251 Nieuwland Science Hall, Notre Dame, IN 46556, USA

U. Möllmann (✉)
Applied Microbiology, Leibniz Institute for Natural Products Research and Infection Biology – Hans-Knoell-Institute, Beutenbergstrasse 11a, 07745 Jena, Germany
e-mail: ute.moellmann@hki-jena.de

Keywords Siderophore synthesis · Hydroxamate · Sugar backbone · Mycobacteria

Introduction

Siderophores are essential for microorganisms to survive in their natural iron limited environment (Boukhalfa and Crumbliss 2002; Winkelmann 2002; Raymond et al. 2003). In the infected host, they represent virulence factors of pathogenic bacteria and fungi (Braun 2005). A variety of artificial siderophores have been synthesized and studied to learn more about the role of siderophores and their specific interactions with microbial iron transport systems (Roosenberg et al. 2000). We were especially interested in the study of mycobacterial siderophores because of the increasing worldwide threat from *M. tuberculosis*. Because mycobacteria have a dense lipophilic outer membrane, they have evolved correspondingly lipid soluble siderophores called the mycobactins to facilitate uptake of iron that is essential for their growth and virulence (Ratledge 2004). Mycobactins contain three bidentate coordinating units, two hydroxamic acids and the combination of a phenol and oxazoline to effectively bind ferric iron. Typically, one of the hydroxamates is cyclic and the other linear with a long hydrophobic acyl side chain. The hydrophobic interaction between the lipophilic mycobactin residues and

the mycobacterial cell envelope facilitates selective siderophore utilization through increased membrane solubility. We had previously demonstrated that incorporation of a long acyl group into peptide-based siderophores promoted their utilization by mycobacteria (Lin et al. 2001) and were interested in determining whether synthetic hydrophobic siderophore analogues with diverse structures might also behave like mycobactins and support the growth of mycobacteria.

The compounds investigated here consist of a core sugar moiety (glucose or mannose) variously substituted with three hydroxamic acids. In a previous paper (Heggemann et al. 2003) we described *retro*-hydroxamate-derived siderophores with a sugar backbone and short alkyl residues. In the work presented here we attached different larger alkyl groups to the chelating termini to learn more about the influence of hydrophobic side chains. Additionally, we prepared both ''normal'' and ''retro'' hydroxamate analogs to investigate the potential influence of the hydroxamate orientation and lipophilicity on iron chelation and siderophore activity.

Material and methods

Synthesis of the siderophore analogues

General: ^{1}H- and ^{13}C-NMR spectra were recorded on a Bruker Avance DPX 300 and DRX 500 spectrometer, respectively. The chemical shifts, δ, are given in ppm relative to tetramethylsilane as an internal standard. Mass spectra were obtained using a Finnigan LCQ mass spectrometer in the electron-spray ionization (ESI) mode. Optical rotations were measured using a Kernchen Polarimeter PROPOL. Column chromatography was accomplished using silica gel (Macherey and Nagel, 60 mesh 0.04–0.063 mm). Purification of compounds by preparative HPLC was performed using an ABIMED GILSON apparatus equipped with a 115 UV detector (254 nm). Thin layer chromatography (TLC) was conducted with precoated silica plates (Merck 60 F254) using UV detection. Solvents and reagents used were dried and purified by standard methods. Reactions were normally carried out under argon. Compounds **9** and **12** were synthesized by the method of Chaudhary et al. (Chaudhary and Hernandez 1979) and purified by HPLC (neutral gradient system, from 30:70 to 17:83 (v/v) water:acetonitrile over 25 min, Eurospher 100 C18).

Synthesis of 4-(Benzyloxy-*n*-butyl-carbamoyl)-butyric acid **5a** via **4a**

To a stirred solution of 16.75 g (75 mmol) of *tert*-butyl-*N*-benzyloxycarbamate, **2**, in 75 ml of dry dimethylformamide (DMF), 1.92 g (80 mmol) of sodium hydride was added in portions over 30 min). After 20 min, a clear solution resulted. Then 12.33 g (0.09 mmol) of *n*-butylbromide was added dropwise and the solution was stirred for another 1 h. Sodium bromide precipitated. After quenching with 10 ml of water, the reaction mixture was extracted three times with *n*-hexane. The combined extracts were dried over sodium sulphate, filtered and evaporated. After thoroughly drying *in vacuo*, 21.1 g (100%) of an analytically pure colourless oil was obtained.

^{1}H-NMR ($CDCl_3$): 7.26–7.42 (m, 5H), 4.80, (s, 2H), 3.39 (t, J = 7.3 Hz, 2H), 1.5–1.69 (m, 2H), 1.48 (s, 9H), 1.22–1.37 (m, 2H), 0.88 (t, J = 7.3 Hz, 3H); ^{13}C-NMR ($CDCl_3$): 156.6, 135.8, 129.3, 128.4, 81.0, 76.8, 49.4, 29.2, 28.3, 19.9, 13.7.

The resulting oil was dissolved in 200 ml of methylene chloride and treated with 45 ml of trifluoroacetic acid (TFA). After stirring over night, the solvent and the TFA were evaporated. The residue was mixed three times with toluene, evaporated for complete elimination of free TFA and dried under *vacuo*. ESI-MS of 4a: *m/z* 180.2 $[M+H]^+$, ^{1}H-NMR ($CDCl_3$): 10.88 (s, br), 7.32–7.41 (m, 5H), 5.07 (s, 2H), 3.26 (m, 2H), 1.70 (m, 2H), 1.36 (m, 2H), 0.91 (t, J = 7.4 Hz, 3H); ^{13}C-NMR ($CDCl_3$): 132.0, 130.0, 129.4, 129.0, 76.7, 49.8, 25.5, 19.6, 13.3.

This oil and 8.6 g (0.075 mol) of glutaric anhydride were dissolved in 150 ml of methylene chloride. Triethylamine (30 ml) was added dropwise over 15 min to the solution. The reaction mixture was stirred for 5 h and kept over night under slightly basic conditions. After cooling to 0°C the mixture was acidified with 2 N HCl, evaporated and extracted three times with 100 ml of ethylacetate. The combined organic layers

were thoroughly washed with brine, dried over sodium sulphate, filtered, evaporated and finally dried under *vacuo* to give 18.19 g (83% in three steps) of slightly brownish viscous oil.

ESI-MS (NH_4OAc) *m/z*: 294.3 $[M+H]^+$, ^{1}H-NMR (500 MHz, DMSO-d_6): 7.34–7.39 (m, 5H), 4.83, (s, 2H), 3.58 (t, J = 6.9 Hz, 2H), 2.40 (t, 7.2 Hz, 2H), 2.20 (t, J = 7.2Hz, 2H), 1.64–1.72 (m, 2H), 1.45–1.53 (m, 2H), 1.18–1.27 (m, 2H), 0.85 (t, J = 7.2 Hz, 3H); ^{13}C-NMR (DMSO-d_6): 174.2, 173.0 (br), 134.9, 129.3, 128.6, 128.4, 75.3, 44.0, 32.9, 30.6, 28.5, 19.6, 19.3, 13.5.

Synthesis of 4-(benzyloxy-cyclohexyl-carbamoyl)-butyric acid (**5b**) was analogous to **5a**

ESI-MS *m/z*: 320.4 $[M+H]^+$ ^{1}H-NMR (d_6-DMSO-d_6): 12.03 (s, br, 1H), 7.31–7.46 (m, 5H), 4.85 (s, 2H), 3.96–4.11 (m, 1H), 2.41–2.51 (m, 2H), 2.18–2.27 (m, 2H), 1.50–1.90, 1.00–1.35 (m, 12 H); ^{13}C-NMR (DMSO-d_6): 174.7 (br),174.2, 135.0, 129.4, 128.6, 128.5, 78.4, 57.4, 32.9, 31.4, 29.7, 25.3, 25.0, 19.6.

Synthesis of 4-(*N*-Benzyloxypropionylamino)-butyric acid (**8**)

A suspension of 15.96 g (0.10 mol) of *O*-benzylhydroxylamine hydrochloride and 28 ml of triethylamine in 250 ml of tetrahydrofuran was cooled to 0°C. Propionyl chloride (8.7 ml, 0.1 mol) was added dropwise. The solution was then allowed to warm to ambient temperature and stirred vigorously for 16 h. The resulting precipitate was separated by filtration. The volatiles were evaporated and the residue was dissolved in 80 ml of ethylacetate. The organic layer was washed with 30 ml of water and twice with 30 ml of brine, dried over sodium sulphate, filtered and evaporated to give 16.79 g (94%) of pure (analytical HPLC) *N*-benzyloxy propionamide (**6**). A portion (1.79 g, 10 mmol) was dissolved in 10 ml of dry DMF and cooled to 0°C. Under stirring, 240 mg (10 mmol) of sodium hydride was added in portions. After a few minutes, a clear solution resulted which was stirred for 1 h. Then a solution of 1.95 g (10 mmol) of ethyl 4-bromobutyrate in 5 ml of DMF was added dropwise and stirred for another hour. This solution was warmed up to ambient temperature and, after stirring for 2.5 h, the solution was acidified with 2 N HCl. The solvent was then evaporated under reduced pressure. The resulting oil was extracted with 3 × 30 ml of ethylacetate. The combined organic extracts were washed with water and brine, dried over sodium sulphate, filtered and evaporated under reduced pressure to give 2.72 g of crude product. After normal phase chromatography (silica gel 60, 0.04–0.063, 350 × 25 mm), 505 mg (17%) of pure 4-(*N*-benzyloxypropionylamino)-butyric acid ethyl ester **7** was obtained. ESI-MS *m/z*: 609.1 $[2M+Na]^+$, 316.5 $[M+Na]^+$ ^{1}H-NMR ($CDCl_3$): 7.34–7.37 (m, 5H), 4.79 (s, 2H), 4.09 (q, J = 7.1 Hz, 2H), 3.67 (t, J = 7.0 Hz, 2H), 2.41 (q, J = 7.5 Hz, 2H), 2.30 (t, J = 7.4 Hz, 2H), 1.88–199 (m, 2H), 1.21 (t, J = 7.1 Hz, 3H), 1.08 (t, J = 7.5 Hz, 3H); ^{13}C-NMR ($CDCl_3$): 175.6 (br), 172.9, 134.5, 129.1, 128.9, 128.7, 76.3, 60.3, 44.9 (br), 31.4, 25.7, 22.3, 14.2, 8.7.

The crude product (485.6 mg, 1.65 mmol) was dissolved in 2 ml of methanol and 2 ml of tetrahydrofuran. To the stirring mixture, 3 ml of lithium hydroxide (2 N) was added. After 1 h, the volatile solvents were evaporated and the residue was acidified with 1 N HCl. The organic phase was extracted with 25 ml of ethylacetate (three times), the combined extracts were washed subsequently with water and brine, dried over sodium sulphate, filtered and concentrated to give 0.472 g (100%) of **8** as a viscous oil. ESI-MS *m/z*: 264.1 $[M-H]^-$, ^{1}H-NMR ($CDCl_3$): 7.32–7.38 (m, 5H), 4.80 (s, 2H), 3.70 (t, J = 6.8 Hz, 2H), 2.32–2.47 (m, 4H), 1.95 (m, 2H), 1.09 (t, J = 7.5 Hz, 3H); ^{13}C-NMR ($CDCl_3$): 177.4, 176.0 (br), 134.4, 129.1, 128.9, 128.7, 76.4, 44.8 (br), 31.1, 25.6, 22.2, 8.7.

Methyl 2,3,4-tris-*O*-[4-(*N*-benzyloxy-*N*-*n*-butylcarbamoyl)-*n*-butyryl]-6-*O*-trityl-α-D-glucopyranoside (**10a**)

Dicyclohexylcarbodiimide (5 g, 24.3 mmol) was added at 0°C to a solution of methyl 6-*O*-trityl-α-D-glucopyranoside (**9**) (2.18 g, 5 mmol), 4-(benzyloxy-*n*-butyl-carbamoyl)-butyric acid (5.87 g, 20 mmol) and *N*,*N*-dimethylaminopyridine (DMAP, 0.1 g) in dichloromethane (300 ml) under stirring. The reaction mixture was stirred

for 1 h at 0°C and for 48 h at ambient temperature. Then the precipitated dicyclohexylurea was filtered and the solvent was evaporated. The residue was dissolved in 200 ml of ethyl acetate. The solution was washed with brine and water, dried over Na_2SO_4, filtered and evaporated. The obtained **10a** (8.16 g, 0.59 mmol, 87%) was a colourless foam in sufficient purity (analytical HPLC) for subsequent use. ESI-MS *m/z* 1262 $[M+H]^+$, 1284 [M+Na].

Methyl 2,3,4-tris-*O*-[4-(*N*-benzyloxy-*N*-*n*-butylcarbamoyl)-*n*-butyryl]-α-D-glucopyranoside (**11a**)

Compound **10a** (3.76 g, 2.98 mmol) was dissolved in dichloromethane (50 ml) and a mixture of 300 µl of boron trifluoride etherate and 5 ml of methanol was added at rt. After 1 h, another 200 µl of boron trifluoride etherate and 3 ml of methanol were added. After 3 h, no starting material remained based on TLC analysis (3:1:0.3-chloroform:ethyl acetate:acetic acid). Then water (10 ml) was added. The organic phase was dried over Na_2SO_4, filtered and evaporated. From 3.18 g of crude product, a 2.5 g portion was purified using normal phase silica gel chromatography (chloroform–ethylacetate, 400 × 45 mm column size) to give **11a** (1.156 g, 48%) as an oil. $[\alpha]^D_{20}$ + 41.46° (c 10.0, methanol). ESI-MS *m/z* 1041.8 $[M+Na]^+$, ^{1}H-NMR ($CDCl_3$): 7.30–7.40 (m, 15H), 5.51 (t, J = 9.7 Hz, 1H), 4.99 (t, J = 9.8 Hz, 1H), 4.92 (d, J = 3.6 Hz, 1H), 4.74–4.84 (m, 7H), 3.45–3.76 (m, 9H), 3.32 (s, 3H), 2.19–2.58 (m, 12 H), 1.74–1.95 (m, 6H), 1.49–1.63 (m, 6H), 1.20–1.35 (m, 6H), 0.83–0.92 (m, 9H); ^{13}C-NMR ($CDCl_3$): 173.5 (br), 172.7, 172.4, 172.1, 134.6, 134.5, 129.0, 128.83, 128.79, 128.6, 96.8, 76.2, 71.0, 69.6, 69.3, 68.8, 60.9, 55.3, 45.3, 33.3, 33.2, 33.1, 31.2, 31.1, 28.9, 19.9, 19.8, 19.7, 19.6, 13.7.

Methyl 2,3,4-tris-*O*-[4-(*N*-hydroxy-*N*-*n*-butylcarbamoyl)-*n*-butyryl]-α-D-glucopyranoside (**1a**)

Compound **11a** (0.55 g, 0.54 mmol) was dissolved in 15 ml of methanol and hydrogenated for 2 h with H_2-Pd/C (10%, 20% w/w) at ambient temperature and atmospheric pressure to give a yellow oil (0.359 g, 89%). $[\alpha]^D_{20}$ + 63.19°. ESI-MS *m/z* 750 $[M+H]^+$, 772 $[M+Na]^+$. ^{1}H-NMR (DMSO-d_6): 9.52 (s, 3H), 5.31 (t, J = 9.8, 1H), 4.95 (t, J = 9.8, 1H), 4.89 (d, J = 3.41), 4.8 (1H, nr), 4.78 (dd, J = 10.33, J = 3.48, 1H), 3.66 (m, 1H), 3.46 (m, 2H), 3.46 (m, 6H, NCH_2), 3.32 (s, 3H, OCH_3), 2.23–2.34 (m, 12H, CH_2), 1.67 (m, 6H, CH_2), 1.47 (m, 6H, CH_2), 1.23 (m, 6H, CH_2), 0.85 (t, 9H, CH_3); ^{13}C-NMR (DMSO-d_6): 172.03, 172.0, 171.9 (br), 171.5, 96.0, 70.2, 69.8, 69.5, 68.3, 59.8, 54.7, 46.8, 32.8, 32.7, 30.7, 30.6, 30.5, 28.4, 19.6, 19.3, 13.6.

Methyl 2,3,6-tris-*O*-[4-(*N*-benzyloxy-*N*-*n*-butylcarbamoyl)-*n*-butyryl]-α-D-glucopyranoside (**11b**) was prepared analogously to **11a** from 3.84 g (3 mmol) of **10a**, but with purification of the product by RP-18 HPLC (gradient system beginning with 37% water to 83% ACN/17% water over 20 min, r_t=39–42 min). Compound **11b** (0.8 g, 26%) was obtained as a colourless oil. $[\alpha]^D_{20}$ + 42.34° (c 10.0, methanol). ESI-MS *m/z* 1020 $[M+H]^+$, 1042 $[M+Na]^+$. ^{1}H-NMR ($CDCl_3$): 7.30–7.40 (m, 15H), 5.32 (t, J = 9.5Hz, 1H), 4.73–4.86 (m, 8H), 4.32 (d, J = 3.5 Hz, 2H), 3.81 (d, t, J = 10 Hz, J = 3.5 Hz, 1H), 3.45–3.75 (m, 7H), 3.30 (s, 3H), 2.19–2.50 (m, 12 H), 1.76–2.00 (m, 6H), 1.50–1.63 (m, 6H), 1.19–1.34 (m, 6H), 0.84–0.91 (m, 9H); ^{13}C-NMR ($CDCl_3$): 173.8 (br), 173.2, 172.9, 172.5, 134.4, 129.0, 128.8, 128.6, 96.7, 76.1, 72.8, 70.7, 69.3, 68.9, 63.0, 55.0, 45.1 (br), 33.7, 33.3, 33.2, 31.2, 31.1, 28.9, 19.9, 19.8, 19.7, 13.7.

Methyl 2,3,6-tris-*O*-[4-(*N*-hydroxy-*N*-*n*-butylcarbamoyl)-*n*-butyryl]-α-D-glucopyranoside (**1b**) was prepared analogously to 1a from **11b** and obtained as a colourless oil in 91% yield. $[\alpha]^D_{20}$ + 49.11° (c 10 methanol). ESI-MS: *m/z* 750 $[M+H]^+$, 772 $[M+Na]^+$. ^{1}H-NMR (DMSO-d_6): 9.56 (s, 3H), 5.65 (1H, br), 5.16 (dd, J = 9.7, 1H), 4.81 (d, J = 4.1, 1H), 4.65 (dd, J = 10.4, J = 3,5, 1H), 4.30 (dd, J = 10.3, 1H), 4.11 (dd, J = 12.0, J = 6.2, 1H), 3.67 (m, 1H), 3.46 (m, 7H, NCH_2, nr), 3.29 (s, 3H, OCH_3), 2.21–2.43 (m, 12H, CH_2), 1.63–1.76 (m, 6H, CH_2), 1.42–1.52 (m, 6H, CH_2), 1.18–1.28 (m, 6H, CH_2), 0.85 (t, J = 7.2 Hz, 9H, CH_3); ^{13}C-NMR (DMSO-d_6): 172.6, 172.2, 172.1, 172.0, 96.1, 71.7, 70.5, 67.8, 62.8, 54.5, 46.7, 33.0, 32.9, 32.7, 30.7, 30.6, 28.4, 19.7, 19.6, 19.3, 13.6.

Methyl 2,3,4-tris-*O*-[4-(*N*-benzyloxy-*N*-cyclohexylcarbamoyl)-*n*-butyryl]-6-*O*-trityl-α-D-glucopyranoside (**10c**) was prepared analogously to **10a** from 0.798 (2.5 mmol) of **5b** and 0.218 g (0.5 mmol) of **9**. The product was obtained in quantitative yield. ESI-MS: *m/z* 1362.4 $[M+Na]^+$.

Methyl 2,3,4-tris-*O*-[4-(*N*-benzyloxy-*N*-cyclohexylcarbamoyl)-*n*-butyryl]-α-D-glucopyranoside (**11c**) was prepared analogously to **11a** from crude **10c**. After purification by NP column chromatography (ethyl acetate/hexanes, 2:1), 0.24 g of **11c** (44% in two steps) was obtained as a colourless oil. ESI-MS: *m/z* 1120 $[M+Na]^+$. ^{1}H-NMR (DMSO-d_6): 7.33–7.44 (m, 15H), 5.32 (t, J = 9.8 Hz, 1H), 4.96 (t, J = 9.7 Hz, 1H), 4.74–4.90 (m, 8H), 3.93–4.09 (m, 3H), 3.65 (m, 1H), 3.32–3.52 (m, 2H), 3.29 (s, 3H), 2.13–2.53 (m, 12 H), 1.44–1.80 (m, 24H), 0.9–1.34 (m, 12H); ^{13}C-NMR (DMSO-d_6): 171.9, 171.4, 134.9, 128.9, 128.5, 128.4, 95.9, 78.3, 70.1, 69.72, 69.65, 68.3, 59.8, 54.6, 33.3, 32.6, 32.5, 31.2, 31.1, 29.7, 25.3, 25.0, 24.9, 24.4, 19.5.

Methyl 2,3,4-tris-*O*-[4-(*N*-hydroxy-*N*-cyclohexylcarbamoyl)-*n*-butyryl]-α-D-glucopyranoside (**1c**) was prepared analogously to **1a** from **11c** as colourless foam, yield 83.4%. $[\alpha]D^{20}$ + 55.16° (c 10.0, Methanol). ESI-MS: *m/z* 828.2 $[M+H]^+$, 849.8 $[M+Na]^+$. ^{1}H-NMR (DMSO-d_6, 500 MHz): 9.24, 9.22 (s, 3H, NOH), 5.30 (dd, J = 9.9, 1H, H-3), 4.94 (t, J = 9.8, 1H, H-4), 4.88 (d, J = 3.4, 1H, H-1), 4.8 (1H, nr, 6-OH), 4.75–4.81 (m, 1H, H-2), 4.10 (m, 3H, NCH_2), 3.65 (m, 1H, H-5), 3.47 (m, 1H, H-6), 3.39 (m, 1H, H-6), 3.32 (s, 3H, OCH_3), 2.17–2.37 (m, 12H, CH_2), 0.98–1.75 (m, 36H) ^{13}C-NMR (DMSO-d_6): 172.02, 172.0, 171.7 (br), 171.5, 95.9, 70.1, 69.8, 69.5, 68.3, 59.8, 53.8, 33.3, 32.8, 32.6, 31.0, 30.9, 28.9, 25.0, 19.5.

Methyl 2,3,4-tris-*O*-[4-(*N*-Benzyloxypropionylamino)-butyryl]-6-*O*-trityl-α-D-glucopyranoside (**10d**) was prepared analogously to **10a** from 0.774 (2.92 mmol) of **8** and 0.318 g (0.73 mmol) of **9**. After NP-chromatography (chloroform/methanol 95/5, 280 × 25 mm) an 87% yield of pure **10d** was obtained. ESI-MS: *m/z* 1200.5 $[M+Na]^+$.

Methyl 2,3,4-tris-*O*-[4-(*N*-Benzyloxypropionylamino)-butyryl]-α-D-glucopyranoside (**11d**) was prepared analogously to **11a** from 0.675 g of **10d**. After purification by NP column chromatography (chloroform/methanol 99/1–95/5) 0.436 g of **11d** (82%) was obtained as colourless oil. ^{1}H-NMR ($CDCl_3$): 7.31–7.39 (m, 15H), 5.48 (t, J = 9.8 Hz, 1H), 5.03 (t, J = 9.7 Hz, 1H), 4.93 (d, J = 3.6 Hz, 1H), 4.84 (dd, J = 10.1 Hz, J = 3.6 Hz), 4.74–4.78 (m, 6H), 3.42–3.81 (m, 9H), 3.43 (s, 3H), 2.18–2.44 (m, 12 H), 1.77–1.97 (m, 6H), 1.01–1.10 (m, 9H); ^{13}C-NMR ($CDCl_3$): ^{13}C-NMR ($CDCl_3$): 175.6 (br), 172.2, 172.0, 171.9, 134.5, 134.4, 128.7–129.1 (nr), 96.7, 76.3, 71.0, 70.0, 69.4, 69.0, 61.0, 55.3, 44.7 (br), 33.9, 31.2, 31.0, 30.8, 25.6, 25.5, 24.9, 22.3, 22.2, 22.0, 8.7.

Methyl 2,3,4-tris-*O*-[4-(*N*-hydroxypropionylamino)-butyryl]-α-D-glucopyranoside (**1d**) was prepared analogously to **1a** from **11d** as colourless foam, yield 86%. ESI-MS: *m/z* 666.8 $[M+H]^+$, 688.7 $[M+Na]^+$. ^{1}H-NMR (DMSO-d_6, 500 MHz): 9.58 (s, 3H, br, N-OH), 5.30 (dd, J = 9.9, 1H, H-3), 4.95 (dd, J = 9.8, 1H, H-4), 4.87 (d, J = 3.4, 1H, H-1), 4.78 (dd, J = 10.0, 3.4, 1H, H-2), 4.78 (1H, nr, 6-OH), 3.65 (m, 1H), 3.43–3.50 (m, 6H), 3.33 (s), 3.32–3.52 (m, 2H, nr), 2.16–2.37 (m, 12H), 1.63–1.78 (m, 6H), 0.92–0.98 (m, 9H). ^{13}C-NMR (DMSO-d_6) 173.7 (br), 171.9, 171.8, 171.3, 95.9, 70.2, 69.9, 69.8, 68.4, 59.8, 54.7, 46.5 (br), 30.3, 30.5, 30.5, 24.9, 21.8 (br), 8.8.

Methyl 2,3,4-tris-*O*-[4-(*N*-Benzyloxypropionylamino)-butyryl]-α-D-glucopyranoside (**11e**) was prepared analogously to **11a** from 0.32 g (3 mmol) of **10d**, but with purification of the product by RP-18 HPLC (gradient system beginning with 37% water to 83% ACN/17% water over 20 min., r_t = 39–42 min). Product 11e (0.105 g, 42%) was obtained as a colourless oil. ESI-MS: 936.6 $[M+H]^+$, 958.5 $[M+Na]^+$], $^{+1}$H-NMR ($CDCl_3$): 7.30–7.40 (m, 15H), 5.43 (1H, t, J = 9.7 Hz), 5.04 (1H, t, 9.8 Hz), 4.99 (1H, d, J = 3.7 Hz), 4.90 (dd, J = 10.1 Hz, J = 3.6 Hz, 1H), 4.78, 4.74, 4.72 (s, 6H), 3.90 (d, t, J = 10.2 Hz, J = 4 Hz, 1H), 3.66 (t, J = 6.9 Hz, 2H), 3.58 (t, d, J = 7 Hz, J = 2 Hz, 2H), 3.48 (t, J = 7.1 Hz, 2H), 3.42 (s, 3H), 3.07–3.13 (m, 2H), 1.56–2.46 (m, 20 H), 0.97–1.13 (m, 9H), ^{13}C-NMR ($CDCl_3$): 175.5 (br), 172.1, 171.9, 171.1, 134.4, 129.0, 128.8, 96.4, 76.2, 71.0, 70.4, 69.0, 68.5, 62.2.0, 55.1, 44.7 (br), 31.2, 31.0, 30.96, 25.6, 22.2, 22.1, 22.05, 8.7.

Methyl 2,3,6-tris-*O*-[4-(*N*-hydroxypropionylamino)-butyryl]-α-D-glucopyranoside (**1e**) was prepared analogously to **1a** from **11e** in 100%

yield. ESI-MS: *m/z* 688.5 $[M+Na]^+$, ^{1}H-NMR (DMSO-d_6): 9.60 (s, 3H, br), 5.63 (1H, br), 5.16 (t, J = 9.8 Hz, 1H, H-3), 4.80 (d, J = 3.5, 1H, H-1), 4.67 (dd, J=10.3, 3.5, 1H, H-2), 4.30 (dd, J = 11.8, 1H), 4.13 (dd, J = 11.9 Hz, J = 5.9 Hz, 1H), 3.68 (m, 1H), 3.42–3.55 (m, 7H, NCH_2), 3.30 (s, 3H), 2.22–2.38 (m, 12H), 1.62–1.84 (m, 6H), 0.96 (t, J = 7.5 Hz, 9H). ^{13}C-NMR (DMSO-d_6) 173.7 (br), 172.4, 172.0, 171.9, 96.2, 71.9, 69.4, 67.8, 62.8, 54.6, 46.5 (br), 30.7, 30.6, 30.4, 24.9, 21.9, 21.8, 8.8.

Methyl 2,3,4-tris-*O*-[4-(*N*-Benzyloxypropionylamino)-butyryl]-6-*O*-trityl-α-D-mannopyranoside (**10f**) was prepared analogously to **10a** from **8** and **12**. After NP-chromatography (chloroform/methanol 99/1) 80.4% of pure **10f** was obtained. ESI-MS: *m/z* 1200.7 $[M+Na]^+$.

Methyl 2,3,4-tris-*O*-[4-(*N*-Benzyloxypropionylamino)-butyryl]-α-D-mannopyranoside (**11f**) was prepared analogously to **11a** from 0.333 g of **10f**. After purification by NP column chromatography (chloroform/methanol 99/1) 0.184 g of **11f** (69.4%) was obtained as a colourless foam. ESI-MS: *m/z* 958.7 $[M+Na]^+$. ^{1}H-NMR ($CDCl_3$): 7.33–7.39 (m, 15H), 5.18–5.39 (m, 3H), 4.75–4.80 (m, 6H), 4.68 (d, J = 1.6 Hz, 1H), 3.50–3.90 (m, 9H), 3.37 (s, 3H), 2.18–2.45 (m, 12 H), 1.80–1.98 (m, 6H), 1.01–1.11 (m, 9H) ^{13}C-NMR ($CDCl_3$): 172.4, 172.0, 171.9, 134.5, 134.4, 129.2, 129.1, 129.0, 128.9, 128.73, 128.70, 128.67, 98.5, 76.3, 70.8, 69.8, 69.2, 66.5, 61.3, 55.2, 44.8 (br), 31.2, 31.1, 31.0, 25.7, 25.6, 22.2, 22.15, 22.11, 8.7.

Methyl 2,3,4-tris-*O*-[4-(*N*-hydroxypropionylamino)-butyryl]-α-D-mannopyranoside (**1f**) was prepared analogously to **1a** from 0.129 g of **11f** as a colourless foam, yield 97%. ESI-MS: *m/z* 689.2 $[M+Na]^+$. ^{1}H-NMR (DMSO-d_6): 9.60 (s, 3H, br, N-OH), 5.07–5.10 (m, 3H), 4.72 (m, 1H), 3.20–3.69 (m, 12H), 2.14–2.41 (m, 12H), 1.64–1.81 (m, 6H), 0.90–0.99 (m, 9H). ^{13}C-NMR (DMSO-d_6) 173.7 (br),171.81, 171.78, 171.5, 97.5, 70.8, 69.0, 68.8, 65.7, 60.2, 54.5, 46.5, 30.6, 30.5, 24.9, 21.9, 21.6, 8.8.

Preparation of iron complexes, determination of their ligand: iron ratio and complex stability by ESI-MS

We investigated the formation and the stability of the iron complexes under in vitro conditions. Complexes were prepared by mixing equimolar amounts of $FeCl_3 \cdot 6H_2O$ (1mmol in water) with the ligand (1 mmol in methanol). As a control to determine if the acidic effects of ferric chloride might be detrimental, we also prepared the complexes using ferric acetylacetonate. Ligand saturation was determined by CAS assays. Free ligands induce a colour change of the CAS medium from blue to orange, but iron saturated ligands do not.

To identify the ratio of complex formation (1:1 or 1:2), 40 µl of the resulting brown solutions were diluted with 200 µl of methanol and 50 µl of the resulting solution was analysed by electrospray MS to determine the stoichiometry of iron binding. For investigation of complex and ligand stability, 20 µl of the same solutions were mixed with 20 µl of potassium dihydrogenphosphate buffer (0.03% w/v) and subjected to ESI-MS analysis either immediately, after 4 h or 16 h.

*c*log*P* values

Log*P* values were calculated using the relevant function of ChemDraw 8.0

Bacterial strains

The mycobacteria studied represent wild type strains (*M. smegmatis* SG 987, from the stock of the Hans-Knoell-Institute, Jena, Germany, *M. smegmatis* mc^2155 (Snapper et al. 1990) and mutants thereof in siderophore biosynthesis and transport: (SG 987-M10 and mc^2155-B1: exochelin biosynthesis deleted; mc^2155-M24, mycobactin biosynthesis deleted; mc^2155-M24-B3, exochelin and mycobactin biosynthesis deleted; mc^2155-M24-U3, mycobactin biosynthesis and exochelin permease deleted (Schumann et al. 1998; Schumann and Möllmann 2001).

Siderophore assays

Utilization of siderophores was determined by a growth promotion assay as described (Schumann and Möllmann 2001). Strains were grown for 2 days on Oxoid no. 1 agar, suspended in medium VA (glycerol, 50 ml; NaCl, 8.5 g/l [pH 7.2]), and diluted to the density of a no. 1 McFarland

standard (3×10^8 CFU per ml). A total of 1.5 ml of this suspension was mixed with 99 ml of iron deficient test medium hindering normal bacterial growth prepared as described (Hall and Ratledge 1986) (glycerol, 20 ml; L-asparagine, 5 g; KH_2PO_4, 5 g/l of distilled water [pH 7.5]). After the addition of 20 g of Al_2O_3 and sterilization at 121°C for 15 min, the suspension was filtered and the pH was adjusted to 6.8. A total of 12 g of agar (Oxoid no. 1) was added, and the medium was sterilized again at 121°C for 15 min. Prior to the inoculation, $ZnSO_4 \cdot 7H_2O$, 2.03 mg; $MnSO_4 \cdot 4H_2O$, 0.405 mg; $MgSO_4$, 0.2 mg; $CaCl_2 \cdot 2H_2O$, 1 mg; $Na_2MoO_4 \cdot 2H_2O$, 0.2 mg; $CuSO_4 \cdot 5H_2O$, 0.2 mg; $CoCl_2 \cdot 6H_2O$, 0.4 mg; and EDDHA, 3.6 g, were added to the medium as a filter-sterilized solution. The inoculated media were poured into Petri dishes. Siderophore solutions (2 mM, 5 µl) were applied on paper discs of 6 mm in diameter on the surface of the agar plates. Mycobactin J (Rhone Merieux, Laupheim, Germany) and Ferricrocin (kindly provided by Prof. H.-P. Fiedler, Tübingen, Germany) were used as positive controls. Growth zones surrounding the discs were read after incubation for two days. Determination of the relative iron complexing capacity of the desferri- or ferri-siderophores was performed by the chrome azurol S (CAS) assay (Schwyn and Neilands 1987) and demonstrated by a positive or negative CAS reaction as indicated in Table 2. Plasticware, which is not prone to iron adsorption, was used instead of glassware. Colorimetric methods were used to confirm that the siderophores remained in the desferri-state.

Results and discussion

Chemical synthesis and iron complexation

Six retro-hydroxamate and hydroxamate compounds **1a–f** with potential Fe(III) binding capacity were synthesized (Scheme 1). For the synthesis of retro-hydroxamates **1a–c**, we used previously described methods (Heggemann et al. 2003). For the synthesis of the normal- hydroxamates **1d–f**, a short new synthetic method was developed (Scheme 2).

Surprisingly, besides formation of the intended 2,3,4-substituted glucopyranosides, structurally unexpected 2,3,6-substituted glucopyranosides, represented by structures **1b** and **1e**, were found as by-products and were unambiguously characterized by 2D-NMR spectroscopic methods, including HMQC, HMBC and COSY. Both **1b** and e showed differences in the ^{1}H-NMR and ^{13}C-NMR pattern to the analogous 2,3,4-substituted compounds, **1a** and **1d**. Cross peaks in the COSY spectrum of OH-groups and respective methylene sugar protons indicated for **1a** and **1d** the expected substitution at the C-6-position. (Fig. 1). In **1b** and **1e** we observed coupling between OH-groups and methine sugar protons in the 4-position. The HMBC-spectra of **1a** and **1d** showed a strong correlation between the 4-positioned carbonyl carbons and the respective H-4-signals, just as **1b** and **1e** showed a correlation between the 6-positioned carbonyl carbons and the respective H-6-protons. The formation of the 2,3,6-derived sugar is probably due to a Lewis acid catalysed intramolecular rearrangement. However we found that the intended 2,3,4-compounds **1a** and **1d** can be readily purified by normal phase chromatography, but the unpredicted byproducts **1b** and **1e** were recovered by reverse phase chromatography (ODC).

In retro-hydroxamates **1a–c** the *N*-hydroxy groups are oriented to the end of the chelating units. The nitrogen atoms of the retro-hydroxamates are substituted throughout with alkyl groups of varied chain length or with a cyclohexane moiety. In contrast, in hydroxamates **1d–f** the carbonyl groups are oriented to the end of the chelating units and contain terminal ethyl groups; i.e. the hydroxamate is derived from propionic acid. The sequence of the functional groups (hydroxamate or retro-hydroxamate) and the chain length of the alkyl groups significantly affect the ferric iron coordination ability due to steric interactions (Dhungana et al. 2007). The iron free siderophores are more hydrophilic than their metal complexes due to the strong interaction of the acidic chelating units (carboxylic acids, catecholates, hydroxamates) with highly charged iron(III) (Lin et al. 2001). After the metal is complexed, the most polar groups are oriented towards the inner space of the molecule and the

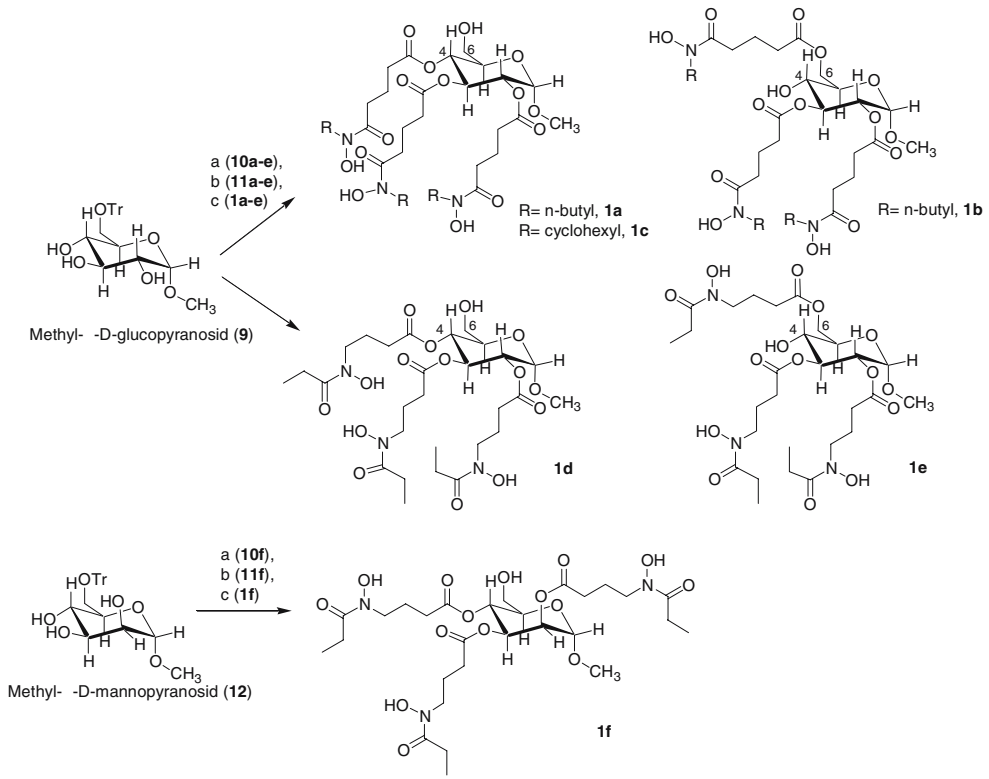

Scheme 1 Synthesis of sugar derived hydroxamate and retro-hydroxamate siderophores (**a**) DMAP, DCC, DCM, **5a**, b or **8**, 16 h (**b**) BF_3OEt_2, DCM, 2 h (**c**) H_2, Pd/C 5%

Scheme 2 Synthesis of hydroxamate moieties (**a**) $(BOC)_2O$, **2** (**b**) NaH, DMF, 3a: BuBr, 3b: CyBr (**c**) TFA, DCM (**d**) Glutaranhydride (**e**) Propionylchloride, TEA, DCM (**f**) NaH, Ethyl-4-Brombutyrate (**g**) LiOH

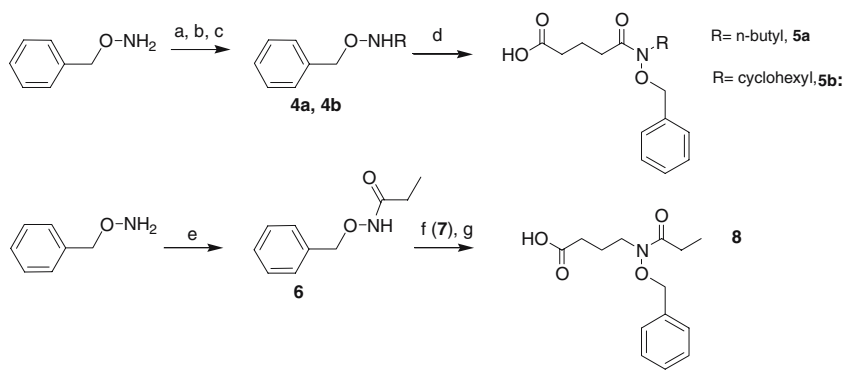

nonpolar moieties, e.g. alkyl spacers, towards the surface of the complex. The 2,3,4- or 2,3,6-substitution pattern of the sugar backbones influences the flexibility of the molecule and consequently the ability of the siderophores to sequester iron(III) (Dhungana et al. 2007).

ESI-MS spectra of the Fe(III) complexes of compounds **1a–f** in methanol or in methanol/potassium dihydrogenphosphate mixture at 0 h[a] revealed that all of the new sugar based siderophores form 1:1 complexes with ferric iron (Table 1). This is consistent with spectrophotometric and potentiometric titration data obtained in aqueous solution for the Fe(III) complex of **1e** and its analogues (Dhungana et al. 2007). In the positive mode we observed strong molecular ion peaks from iron with trischelating ligands and sodium (A) or protons (B), respectively. After 4 h

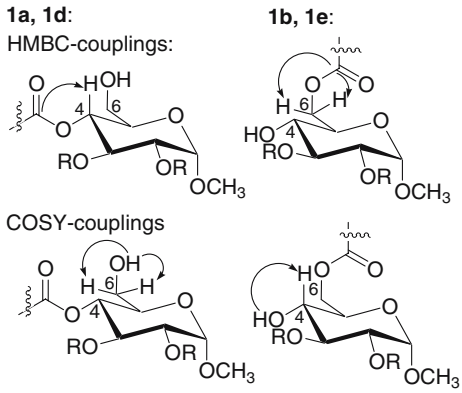

Fig. 1 2-D NMR assignments

and 16 h of reaction with potassium dihydrogenphosphate, compounds, **1a, 1d–e** still showed the same pattern as at 0 h[a], indicating that the siderophore structure and iron coordination did not change. However, when compared to methanol solution, the complexes of **1c–f** in methanol containing aqueous buffer were unstable, as demonstrated by the presence of free ligand (C) and of ligand with one cleaved hydroxamate arm (D) already at 0 h. After 16 h, higher concentrations of the ligand with one cleaved hydroxamate arm were observed for **1b** and **1c**. Compounds **1a** and **1f** showed cleavage of the hydroxamate binding site in aqueous buffer/methanol also, but only in a rather small range and invariant with time. ESI-MS-spectra of all of the ferric complex solutions (**1a–f**) in methanol (0 h[b]) showed small amounts of the ligand with a cleaved hydroxamate arm for **1d** and **1e** only. However, for all siderophore-iron complexes the relative intensity of quasimolecular ions with sodium or hydrogen, respectively, was 100%.

Siderophore activity and clogP values

Siderophore activity was tested using *M. smegmatis* wild type strains and mutants in siderophore biosynthesis and transport (Table 2). This set of wild type strains and mutants differ by the presence or absence of the endogenous siderophores exochelin and mycobactin as well as by the presence or absence of the exochelin permease. By use of these strains in growth promotion experiments, it is generally possible to differentiate between siderophore iron supply processes that include ligand exchange with exochelin and/or mycobactin (strains SG 987, mc^{2}155, SG 987-M10, mc^{2}155-B1, mc^{2}155-M24) and those that exclude ligand exchange (mc^{2}155-M24-B3, mc^{2}155-M24-U3). Additionally, it is possible to differentiate between uptake via the exochelin permease (mc^{2}155-M24-B3) and uptake by an alternative transport system (mc^{2}155-M24-U3). Consistent with previous investigations (Lin et al. 2001) we generally observed stronger growth promotion activity by the iron complexed siderophores compared to their iron free analogues.

Table 1 ESI-MS spectra and iron(III) complex stability

Time	1a	1b	1c	1d	1e	1f
0 h [a]	A (100%) B (15%) D (20%)	A (100%) B (20%) D (10%)	A (100%) C (50%) D (10%)	A (75%) C (100%) D (55%)	A (60%) D (100%)	A (100%) C (80%) D (10%)
4 h [a]	A (100%) B (5%) D (15%)	A (100%) B (15%) D (10%)	A (100%) C (30%) D (10%)	A (100%) C (70%) D (65%)	A (55%) D (100%)	A (100%) C (55%) D (10%)
16 h [a]	A (75%) B (10%) D (20%)	A (100%) B (15%) D (55%)	A (60%) C (85%) D (35%)	A (100%) C (100%) D (55%)	A (65%) D (100%)	A (100%) C (40%) D (10%)
0 h [b]	A (25%) B (100%)	A (15%) B (100%)	B (100%)	A (100%) B (80%) D (20%)	A (100%) B (20%) C (10%) D (20%)	A (100%) B (20%) C (15%)

A = $[L+Fe+Na]^+$, B = $[L+Fe+H]^+$, C = $[L+Na]^+$, D = [L-(hydroxamate-moiety)+Na]$^+$, L = ligand

[a] MeOH/Water (KH_2PO_4, 0.03%) 1:1

[b] In MeOH

Table 2 Growth promotion and CAS activity

Bacterial strains/characteristic compounds	*c*Log*P*	CAS-Assay[c]	*Mycobacterium smegmatis*						
			SG 987	SG 987-M10	mc^2 155	mc^2 155-M24	mc^2 155-B1	$mc^2$155-M24-B3	mc^2 155-M24-U3
Exochelin[a]			+	–	+	+	–	–	+
Mycobactin[a]			+	+	+	–	+	–	–
Exochelin permease[b]			+	+	+	+	+	+	–
1a	5.0679	11	++++	++	++++	–	+++	–	–
1a +Fe^{3+}		0	++++	+++	++++	++++	++++	++	+
1b	5.1144	10	++++	++	++++	–	++++	–	–
1b + Fe^{3+}		0	++++	+++	++++	+++	++++	++	+
1c	6.3999	9	++++	+++	++++	–	++++	–	–
1c + Fe^{3+}		0	+++	+++	+++	++	++	+	+
1d	1.8939	12	+	–	+	–	+	–	–
1d + Fe^{3+}		0	++++	+++	++++	++++	++++	++	++
1e	1.9404	11	+	–	–	–	–	–	–
1e + Fe^{3+}		0	+++	++++	++++	++++	++++	+++	+++
1f	1.7102	14	+	–	+	–	+	–	–
1f + Fe^{3+}		0	+++	+++	++++	+++	++++	+	–
Mycobactin		0	++	++	++	++	++	++	++
Ferricrocin		0	++	++	++	++	+	–	–

[a] Indicates that the strain biosynthesizes the indicated siderophore and has the potential for ligand exchange: yes (+) or no (–)

[b] Uptake of Exochelin by the indicated strain: yes (+) or no (–)

[c] Diameter of orange halo in mm –, +, ++, +++, ++++: Indicates the presence and increasing intensity of growth promoting activity

Nearly zero growth promotion activity was detected for the hydroxamates **1d–f** when applied as desferri-compounds, but strong growth promotion activity was detected when applied as preformed iron complexes. In contrast, the retro-hydroxamates **1a–c** promote growth of the mycobacteria also in the desferri form.

Our results suggest that growth promotion activity depends on lipophilicity rather than on siderophore receptor mediated uptake. It seems reasonable that the higher lipophilic character of the retro-hydroxamates facilitates diffusion into the hydrophobic mycobacterial cell envelope. Siderophore **1c**, the most lipophilic siderophore studied due to the large cyclohexyl groups, exhibits the highest calculated log*P* value (*c*Log*P* = 6.3999). Compared to **1c**, the *c*Log*P* values of **1a** and **1b**, which have terminal butyl groups at the hydroxamate arms instead of the cyclohexyl moiety, are decreased more than one unit on the logarithmic scale. This is reflected by the respective CAS values and growth promotion activity found for this series of relatively hydrophobic and less diffusable analogs as shown in Table 2.

Generally, the *c*Log*P* of the retro-hydroxamates **1a–c** are ca 4 log units higher than the *c*Log*P* of the normal hydroxamates. That characteristic enables the desferri-retro-hydroxamates to diffuse into the hydrophobic mycobacterial cell envelope. However, ligand exchange with the intra-envelope short-term storage molecule mycobactin is necessary to present the Fe(III) to a reductase for conversion to Fe(II). (Ratledge 2004) The ferrous iron (possibly complexed with salicylic acid) will then be shuttled across the membrane into the cytoplasm to support growth. There is no growth promotion of the mycobactin deficient mutants by the desferri-retro-hydroxamates, in contrast to the strong growth promotion of the strains with normal mycobactin biosynthesis. The amount of iron ions transported to the cell wall by the preformed iron complexes of compounds **1a–c** seems to be high enough to support the low affinity high capacity iron uptake pathway (Wheeler and Ratledge et al. 1994).

The propionyl group-containing normal-hydroxamates, **1d–f**, have *c*Log*P* values more than four units lower on the logarithmic scale compared to **1c**. Accordingly, the growth promoting activity without coordinated iron is very low. After complexation, the ionic hydroxamic acid groups are strongly bound to the iron(III) atom and the more lipophilic groups are directed to the outside of the molecule. This enhanced lipophilicity increases growth promotion activity dramatically, supporting the hypothesis described above, that stimulation of growth is due to increased solubility in the hydrophobic cell envelope and release of ferric iron rather than to receptor-mediated uptake. Despite the differences in *c*Log*P*, the lower stability of the iron complexes of the normal-hydroxamates releases sufficient iron to the cell to support the low affinity iron uptake pathway as well.

Interestingly, the glucose based ferri-hydroxamates **1d** and **1e** demonstrated improved growth promoting activity for both of the mutant strains mc^2155-M24-B3 and mc^2155-M24-U3, which are completely blocked in their species specific exochelin/mycobactin iron uptake system. Whereas the mannose based ferri-hydroxamate **1f** and the glucose based ferri-retro-hydroxamates **1a–c** are less effective for exochelin/mycobactin biosynthesis mutant mc^2155-M24-B3, but inactive for the mycobactin biosynthesis/exochelin uptake mutant mc^2155-M24-U3. (Table 2) This apparent activity of the iron complexes of **1d** and **1e** may be due to their lower stability. Slow hydrolytic release of a hydroxamate arm in aqueous buffer (Table 1) would make the iron less tightly bound to the resulting bis-hydroxamate-containing siderophore remnant and kinetically more labile. The iron would then be more available for exchange across the cell membrane. Further synthetic, physicochemical and biological investigations are necessary to explore this hypothesis.

Acknowledgements Financial support by DFG 1213/1-1 (PG and UM), by NSF CHE-0418006 (ALC) and by NIH AI054193 (MJM) is gratefully acknowledged. We thank Renate Heidersbach, Anne Ludwig and Irmgard Heinemann for their excellent technical assistance.

References

Boukhalfa H, Crumbliss AL (2002) Chemical aspects of siderophore mediated iron transport. Biometals 15:325–339

Braun V (2005) Bacterial iron transport related to virulence. In: Russell W et al. (eds) Concepts in bacterial virulence. Karger, Basel, pp 210–233

Chaudhary S, Hernandez O (1979) A simplified procedure for the preparation of triphenylmethylethers. Tetrahedron Lett 20:95–98

Dhungana S, Harrington J, Gebhardt P, Möllmann U, Crumbliss AL (2007) Iron coordination properties of a saccharide based ferrichrome analogue (submitted)

Hall RM, Ratledge C (1986) Distribution and application of mycobactins for the characterization of species within the genus Rhodococcus. J Gen Microbiol 132:853–856

Heggemann S, Möllmann U, Gebhardt P, Heinisch L (2003) Trishydroxamates and triscatecholates based on monosaccharides and myo-inositol as artificial siderophores. Biometals 16:539–51

Lin Y-M, Miller MJ, Möllmann U (2001) The remarkable hydrophobic effect of a fatty acid side chain on the microbial growth promoting activity of a synthetic siderophore. Biometals 14:153–157

Ratledge C (2004) Iron, mycobacteria and tuberculosis. Tuberculosis, (Edinb) 84:110–130

Raymond KN, Dertz EA, Kim SS (2003) Enterobactin: an archetype for microbial iron transport. Proc Natl Acad Sci U S A 100:3584–3588

Roosenberg JM II, Lin YM, Lu Y, Miller MJ (2000) Studies and syntheses of siderophores, microbial iron chelators, and analogs as potential drug delivery agents. Curr Med Chem 7:159–197

Schumann G, Möllmann U (2001) Screening system for xenosiderophores as potential drug delivery agents in mycobacteria. Antimicrob Agents Chemother 45:1317–1322

Schumann G, Möllmann U and Heinemann I, DE (17.4. 1998)

Schwyn B, Neilands JB (1987) Universal chemical assay for the detection and determination of siderophores. Analytic Biochem 160:47–56

Snapper SB, Melton RE, Mustafa, Kieser ST, Jacobs WR (1990) Isolation and characterization of efficient plasmid transformation mutants of Mycobacterium smegmatis. Mol Microbiol 4:1911–1919

Wheeler PR, Ratledge C (1994) Metabolism of *Mycobacterium tuberculosis*. In: Bloom BR (eds) Tuberculosis. ASM Press, Washington, DC, pp 353–385

Winkelmann G (2002) Microbial siderophore-mediated transport. Biochem Soc Trans 30:691–696